Letter to the Editor

Epigallocatechin-3-gallate shows anti-proliferative activity in HeLa cells targeting tubulin-microtubule equilibrium

Subhendu Chakrabarty, Arnab Ganguli, Amlan Das, Debasish Nag, Gopal Chakrabarti[*]

Department of Biotechnology and Dr. B. C. Guha Centre for Genetic Engineering and Biotechnology, University of Calcutta, 35 Ballygunge Circular Road, Kolkata, WB 700019, India

A R T I C L E   I N F O

A B S T R A C T

In this study our main objective was to find out a novel target of the major bioactive green tea polyphenol, Epigallocatechin-3-gallate (EGCG), in cervical carcinoma HeLa cells. We found that EGCG showed antiproliferative activity against HeLa cells through depolymerization of cellular microtubule. EGCG also prevented the reformation of the cellular microtubule network distorted by cold treatment and inhibited polymerization of tubulin in $cell$-$free$ $system$ with IC50 of 39.6 ± 0.63 μM. Fluorescence spectroscopic analysis showed that EGCG prevented colchicine binding to tubulin and in $silico$ study revealed that EGCG bound to the α-subunit of tubulin at the interphase of the α-and β-heterodimers and very close to colchicine binding site. The binding is entropy driven (ΔS^0 was 18.75 ± 1.48 cal K^{-1} mol^{-1}) with Kd value of 3.50 ± 0.40 μM. This is a novel mechanism of antipriliferative activity of EGCG.

© 2015 Elsevier Ireland Ltd. All rights reserved.

1. Introduction

(−)-Epigallocatechin-3-gallate (EGCG), the most abundant and potent tea catechin, has anti-tumor activity against various types of cancers both in $vitro$ and in $vivo$ [1–3]. It shows antiproliferative activity by inducing apoptosis through mitochondrial pathway [4,5] and also by modulating the expression of NF-kB, MAPK, PI-3-K/Akt and p53 [6–8]. EGCG has also been reported to possess anti-inflammatory, anti-oxidative and anti-angiogenic effects [9,10].

Cervical cancer is one of the most common forms of cancers in women. Although it can be prevented and is curable if detected early [11], there is no such treatment for cervical carcinoma. In this regard there is a great need to investigate and identify new agents for the treatment of this disease. There are previous reports that EGCG induces apoptosis, blocks cell cycle at S- and G_2/M phases and shows anti-angiogenic effect in human cervical carcinoma (HeLa) cells [12–14].

In our study, we have found a new mode of action of EGCG in HeLa cells. We examined its antiproliferative activity through its ability to depolymerize cellular microtubule and also found that EGCG inhibited tubulin assembly both in cells and in cell free system. It is now well established that tubulin, a heterodimeric (containing α and β subunits) protein, and its polymer microtubule are popular targets for anticancer drugs [15] and many natural compounds which target the dynamicity of tubulin-microtubule system are in different stages of drug development [16–18]. Although the growth inhibitory effect of EGCG against HeLa cells are well reported, our study specifically suggests that EGCG can interfere the dynamicity of tubulin-microtubule system which may account for its cytotoxicity in HeLa cells. We have also established EGCG-tubulin interaction by measuring various kinetic and thermodynamic parameters. Thus our finding revealed a novel target of EGCG in cervical carcinoma (HeLa) cells.

2. Materials & methods

2.1. Chemicals

DMEM, FBS, penicillin-streptomycin, trypsin, and amphotericin B were purchased from HyClone, Logan, UT, USA. Human cervical carcinoma cells (HeLa) were obtained from National Centre for Cell Science, Pune, India. Mouse monoclonal anti-α-tubulin antibody (sc-5286), mouse monoclonal anti-β-actin antibody (sc-47778), anti-mouse HRP-conjugated IgG antibody (sc-2005), rabbit

polyclonal anti-p21 antibody (sc-397) and goat anti-rabbit HRP-conjugated IgG antibody (sc-2004) were purchased from Santa Cruz Biotechnology and anti-mouse rhodamine conjugated IgG antibody (cat# RTC3) and the Bradford Protein estimation kit were purchased from GENEI, India. DAPI, GTP, PIPES and EGCG were purchased from SIGMA, St. Louis, MO, USA. All other chemicals and reagents were of analytical grade and purchased from Sisco Research Laboratories, India.

2.2. EGCG treatment

Dry powder of EGCG was directly dissolved in water. For cell biology experiments, secondary solution was prepared in PBS. All in vitro experiments were done preparing secondary solutions in PEM buffer (50 mM PIPES, 1 mM EGTA, 1 mM $MgSO_4$, pH 7).

2.3. Cell culture

HeLa cells were maintained in DMEM medium supplemented with 1 mM L-glutamine, 10% fetal bovine serum, 50 μg/ml penicillin, 50 μg/ml streptomycin and 2.5 μg/ml amphotericin B at 37 °C in a humidified atmosphere containing 5% CO_2. Cells were grown in tissue culture flasks until they were 80% confluent before trypsinization with 1 × trypsin and splitting.

2.4. Cell viability assay

The effect of EGCG on the viability of HeLa cells was determined by MTT (3-[4,5-dimethylthiazol-2-yl]-2,5-diphenyltetrazolium bromide) assay [19]. Cells were plated in 96-well culture plate (1 × 10^4 cells per well) and treated with various concentrations of EGCG (0–200 μM) for both 24 h and 48 h. MTT solution (5 mg/ml) was prepared in PBS, filter sterilized, and 20 μl was added to each well. The purple precipitate formed was dissolved in 100 μl Triton-X and the absorbance was measured on an ELISA reader (MultiskanEX, Lab systems, Helsinki, Finland) at a test wavelength of 570 nm and a reference wavelength of 650 nm. Data was analyzed by plotting percent of viable cells against EGCG concentration, considering control cells as 100% viable [20].

2.5. Cell cycle analysis

HeLa cells were grown in 35 mm plate and treated with 50 μM EGCG for 24 h and 48 h. Cells were then harvested and fixed with ice chilled methanol. After removing the fixative cells were incubated with RNase (100 μg/ml) for 4 h at 37 °C. After incubation 50 μg/ml Propidium iodide (PI) was added and cell cycle analysis was performed using the Becton Dickinson FACScan and the data was analyzed by CellQuest program. For each sample, 10,000 cells were counted [20].

2.6. Confocal microscopy

HeLa cells were cultured on cover slips and treated with EGCG (0–100 μM) for 24 h. Subsequently cells were washed with PBS, fixed with 2% paraformaldehyde and permeabilized with cell permeable solution (0.1% Na-Citrate, 0.1% Triton). Nonspecific binding sites were blocked by incubating cells with 5% BSA and then the cells were stained with mouse monoclonal anti-α-tubulin antibody (1:200 dilutions) followed by anti mouse rhodamine conjugated IgG antibody (1:150 dilutions) and DAPI (1 μg/ml). Cellular actin was stained with mouse monoclonal anti-β-actin antibody (1:200 dilutions) followed by anti mouse rhodamine conjugated IgG antibody (1:150 dilutions). Cells were viewed under a Ziess LSM 510 Meta confocal microscope.

2.7. Western blot analysis

Western blot analysis was done to determine the expression of cyclin dependent kinase-2 inhibitor and cell cycle checkpoint protein p21 in EGCG treated and untreated HeLa cells. Cells were incubated with EGCG (0, 25 and 50 μM) for 24 h and then harvested and lysed with ice-cold lysis buffer and cellular protein was isolated by centrifugation at 12000 g for 30 min at 4 °C [20]. Total protein concentration of the supernatant was measured by Bradford method [22] and equal amounts of each sample were electrophoresed in 10% SDS-PAGE and subsequently western blotted and probed with antibody against p21 (1:1000 dilution).

The cellular tubulin polymerization was quantified by a modified method described by Minotti et al. [21]. Cells were treated with 50 μM EGCG and 1 μM colchicine (positive control) for 24 h and harvested by trypsinization. Cells were then processed to separate soluble tubulin from polymerized tubulin [20]. Total protein concentration of both fractions were estimated separately by the Bradford method [22] and equal amounts (50 μg) of each sample were electrophoresed in a 10% SDS-polyacrylamide gel. The sample was then analyzed by Western blotting and probed with the antibody against α-tubulin (1:1000 dilutions).

2.8. Assembly of microtubules after cold treatment in EGCG treated HeLa cells

Cells (1 × 10^5 cells/ml) were grown on glass coverslips for 24 h and then incubated at 4 °C for 6 h. Then the cold medium was replaced with warm medium containing EGCG (0 and 50 μM) and the samples were incubated at 37 °C for 60 min. Cells were then harvested, fixed and microtubule was visualized by immunofluorescence against α-tubulin using a Ziess LSM 510 Meta confocal microscope [20].

2.9. Purification of tubulin from goat brain

Tubulin was isolated from goat brain by two cycles of temperature-dependent assembly and disassembly in PEM buffer (50 mM PIPES, 1 mM EGTA, and 0.5 mM $MgCl_2$, pH 6.9) in the presence of 1 mM GTP, followed by two more cycles in 1 M glutamate buffer [23]. The protein concentration was estimated by Bradford method.

2.10. Microtubule polymerization

Polymerization of tubulin (10 μM) was initiated with 1 mM GTP at 37 °C in polymerization buffer (1 mM $MgSO_4$, 1 mM EGTA, 1.0 M monosodium glutamate, pH 6.8) in presence of EGCG (0–50 μM) and was monitored by light scattering at 350 nm using V-630 Jasco Spectrophotometer connected to constant temperature water circulating bath [24].

2.11. Microtubule pelleting assay

Tubulin (10 μM) was incubated in the absence and presence of EGCG (0–50 μM) at 37 °C in polymerization buffer and microtubule formed was pelleted down by centrifugation in Beckman Coulter Optima MAX-XP Ultracentrifuge using TL 100 rotor. Pellets were resuspended in PEM buffer, electrophoresed in 10% SDS-PAGE and then stained with coomassie blue.

2.12. Association kinetics

Kinetics of EGCG-tubulin binding was monitored by measuring the intrinsic tryptophan fluorescence [25,26] of fixed amount of

tubulin (1 μM) in the presence of excess amount of EGCG (20 μM). The emission of tryptophan fluorescence at 335 nm was measured with time upon excitation at 295 nm using 1 mm excitation and 1 mm emission slits at 25 °C in a fluorescence spectrophotometer (Photon Technology International, Inc. USA, Model QM-4CW). The apparent association rate constant (k_{on}) was obtained according to the methods of Lambier and Engelborghs [27] and others [28].

$$Q_{max} - Q_t = A \cdot e^{-\alpha t} + B \cdot e^{-\beta t}$$

where A and B are amplitudes and α and β are observed rate constants of the fast and slow phases, respectively. The amplitude of the slow phase (B) was low relative to that of the fast phase (A) and the slow phase was not analyzed further. The apparent association rate constants (k_{on}) were calculated by dividing the rate constant of the fast phase (α) by ligand concentration, where α is the slope of the plot of $\ln(Q_{max} - Q_t)$ versus time t [28].

After calculating k_{on} values at different temperatures (22 °C-37 °C), the activation energy was determined by plotting $\ln(k_{on})$ against 1/T according to the Arrhenius equation,

$$k_{on} = Ae^{(-E_A/RT)}$$

where, E_A is the activation energy, R is the gas constant, T is temperature in absolute scale and A is the pre-exponential factor [28].

2.13. Job plot

The stoichiometry of binding was determined using the method of continuous variation [29]. Several mixtures of tubulin and EGCG were prepared by continuously varying concentrations of tubulin and EGCG in the mixture keeping the total concentration of EGCG plus tubulin constant at 5 μM. The reaction solutions were incubated for 30 min at 25 °C, and the quenching of tryptophan fluorescence was recorded at 335 nm using 295 nm as the excitation wavelength.

2.14. Binding constant

To determine the dissociation constant (K_d) of EGCG-tubulin interaction, tubulin (1 μM) was incubated with varying concentrations of EGCG (0–20 μM) at 25 °C for 30 min and intrinsic tryptophan fluorescence at 335 nm was measured. The dissociation constant (K_d) was determined following the relationship [18,26],

$$1/X = 1 + K_d/L_f,$$

where, L_f represents free EGCG concentration, X is the fraction of binding sites occupied by EGCG. X was determined using an equation, $X = (F_0 - F)/F_{max}$, where F_0 is the fluorescence intensity of tubulin in the absence of EGCG, F is the corrected fluorescence
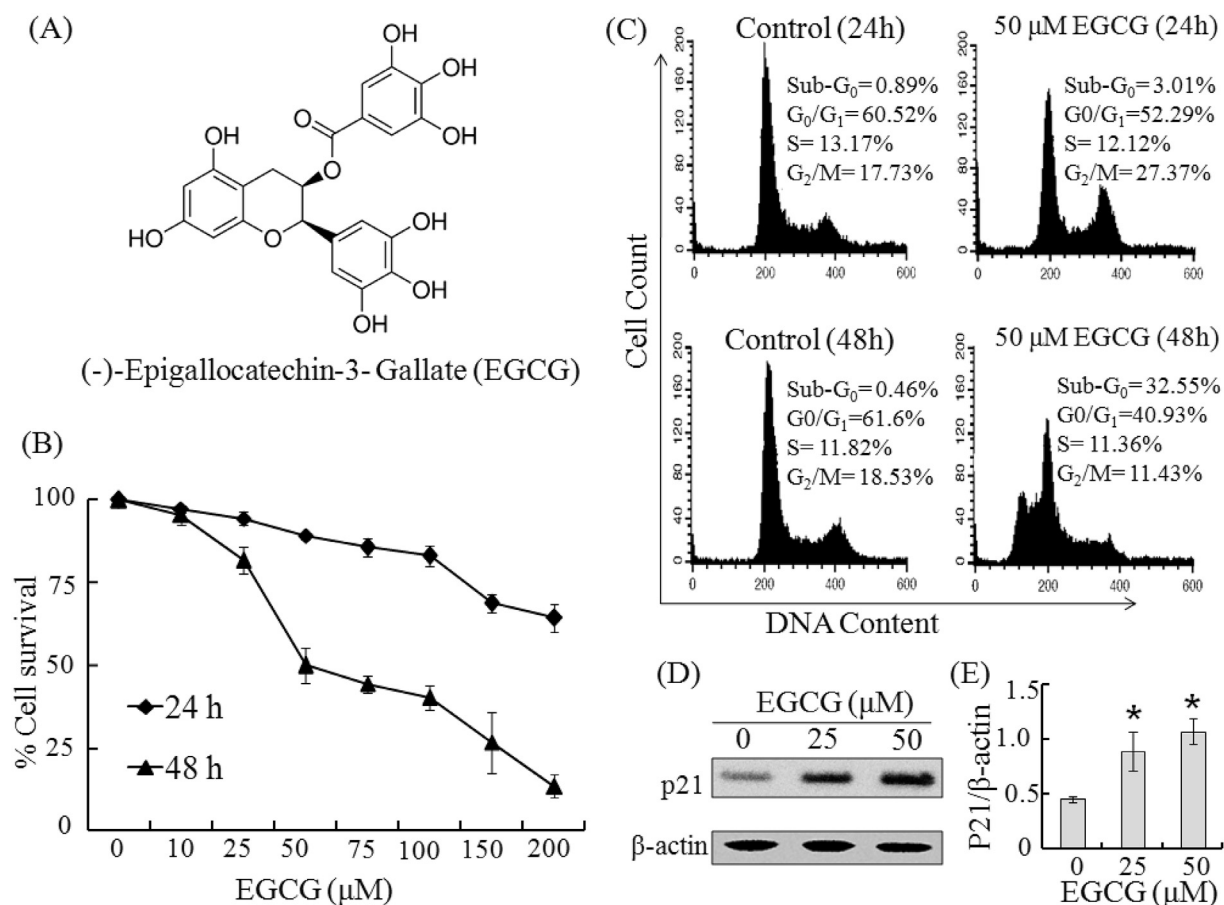
Fig. 1. (A) Chemical structure of EGCG. (B) Effect of EGCG on the viability of HeLa cells (MTT assay). Cells were treated with EGCG (0–200 μM) for 24 and 48 h. The data are shown as mean ± SD. (C) Cell cycle distribution of HeLa cells after treating the cells with 0 and 50 μM EGCG for 24 h (upper row) and 48 h (bottom row). Data shows one of the three individual experiments with similar results. (D) Western blot analysis showing the effect of EGCG (0, 25, 50 μM) on expression of p21. β-actin was used as loading control. (E) Histogram analysis of western blot showing increase of p21 expression quantitatively with increasing doses of EGCG. Data represent mean ± SD (* = p < 0.05 compared to untreated control).

intensity of tubulin in the presence of EGCG, and F_{max} is calculated from the plot of $1/(F_0 - F)$ versus $1/[EGCG]$ and extrapolating $1/[EGCG]$ to zero. L_f was determined by the relationship, $L_f = C - X[Y]$, where C is the total concentration of EGCG and $[Y]$ is the molar concentration of ligand-binding sites using a stoichiometry of 1:1 as determined from the Job plot.

Using same experimental condition, we determined the association constant (K_a) and the number of binding sites of EGCG on tubulin by analyzing the Scatchard equation,

$$r \big/ \left[L_f \right] = nK_a - rK_a,$$

where K_a is the association constant, r is the ratio of the concentration of bound ligand to total tubulin, and n represents the maximum number of ligand binding sites per tubulin dimer. The association constants can be determined from the slope of the plot of $r/[L_f]$ against r, and the number of binding sites can be obtained from the extrapolated value of r at $r/[L_f]$ equals to zero [28].

2.15. Thermodynamic parameters of EGCG binding to purified tubulin

The enthalpy (ΔH^0) and entropy (ΔS^0) of EGCG-tubulin interactions were obtained by plotting log of K_a against $1/T$ according to the van't Hoff's equation, $\ln K_a = -\Delta H^0/RT + \Delta S^0/R$ [28]. Once ΔH^0 and ΔS^0 are known, the free energy change of EGCG-tubulin interaction (ΔG^0) at 25 °C was estimated using the relationship, $\Delta G^0 = \Delta H^0 - T\Delta S^0$.

2.16. Binding site of EGCG on tubulin

To determine whether EGCG binds at the colchicine binding site on tubulin, we measured the inhibition of formation of colchicine-tubulin complex in presence of EGCG taking fluorescence at 430 nm [18]. Tubulin (3 μM) was incubated with different concentrations of EGCG (0–50 μM) at 37 °C for 30 min. Colchicine (5 μM) was added to all the mixtures and incubated further for 30 min at 37 °C and the fluorescence spectrum was recorded using 360 nm as the excitation wavelength.

2.17. In silico prediction of EGCG-tubulin binding

The latest pdb file of tubulin 1jff.pdb was prepared by *CHARMm* forcefield applied *Prepeare Protein* module and ligand was prepared by *Prepeare Ligand* module of discovery studio 2.5. In both cases all parameters were taken as default value (See supplementary data). After determining 42 binding sites on tubulin surface, we used *CDOCKER* module to dock most stable conformation of EGCG on each binding site of tubulin and after that we calculated the binding energy of each docked tubulin-EGCG complex. The lowest binding energy for EGCG binding to tubulin considered as the most stable tubulin-EGCG complex [30,31].
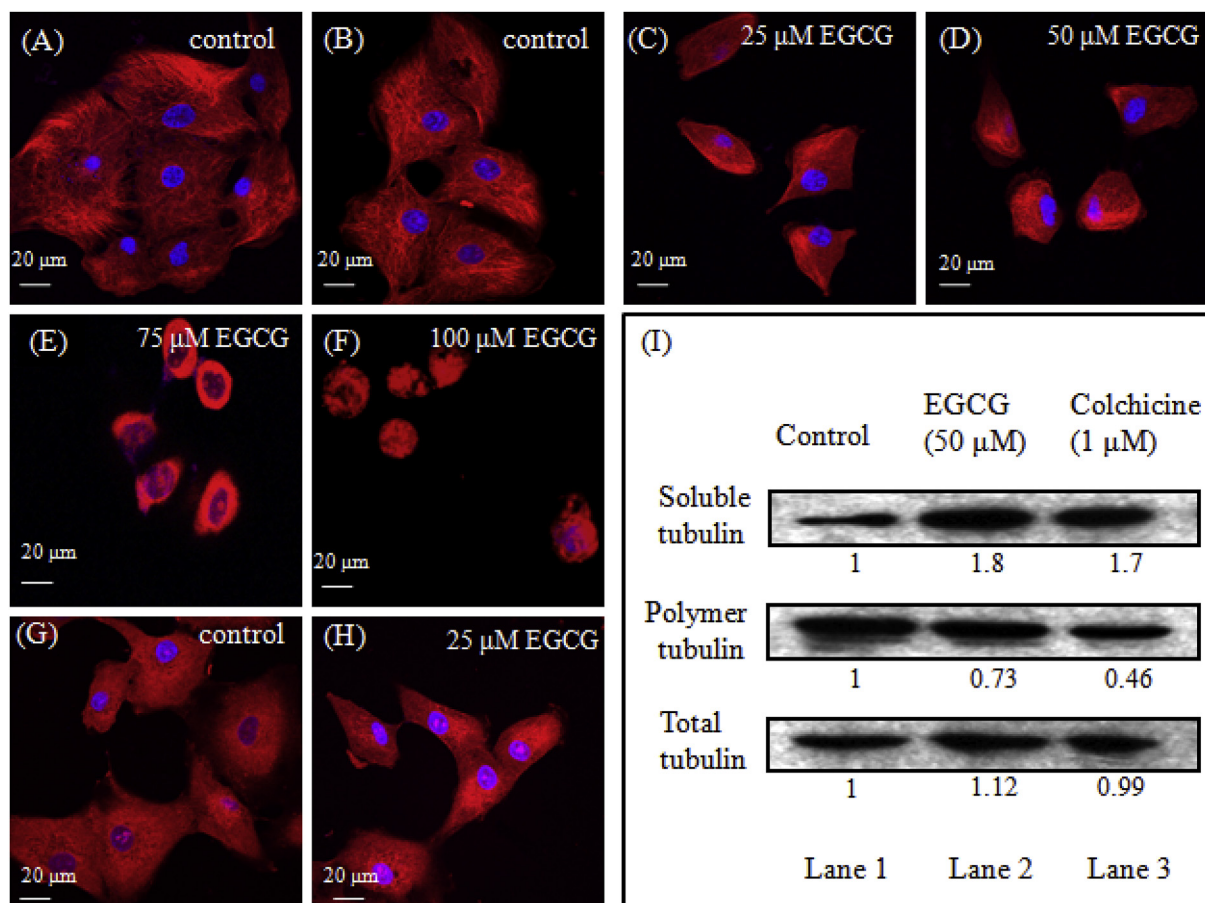
Fig. 2. Immunofluorescence study of disruption of interphase microtubules of HeLa cells treated with EGCG. (A) and (B) are the control cells, (C), (D), (E) and (F) are cells after 24 h treatment with 25, 50, 75 and 100 μM EGCG, respectively. Experiments were repeated thrice with similar results. (G) and (H) are the untreated and 25 μM EGCG treated HeLa cells, respectively, duly stained with anti-β-actin antibody. (E) Western blot analysis showing effect of EGCG on polymerized tubulin in HeLa cells. Cells were treated with 0 μM and 50 μM EGCG and 1 μM colchicine (positive control) for 24 h.

2.18. Statistical analysis

Data are presented as the mean of at least three independent experiments along with standard deviation (SD). Statistical analysis of data was done by Student's t test. Probability values (p) of <0.05 were considered to be statistically significant.

3. Results and discussion

3.1. EGCG inhibited proliferation of HeLa cells and induced cell cycle arrest in G_2/M phase

Previous reports show wide range of IC50 values of EGCG against different cell lines in both 24 h and 48 h [3,12−14]. To determine the effect of EGCG on the viability of HeLa cells under our experimental conditions, we performed MTT assay. After 24 h of treatment, maximum 35% cell death was observed at 200 μM dose. On the other hand, a large amount of reduction in cell viability was observed (upto 87%) after 48 h treatment with an IC_{50} value of 54 ± 6.02 μM (p < 0.01) (Fig. 1B). The IC_{50} value we observed in 48 h is in very good agreement with that previously reported in HeLa cells [14].

Cell cycle analysis showed that 24 h treatment with 50 μM EGCG caused G_2/M arrest without any significant cell death, accumulating 27.37% cells in G_2/M phase compared to 17.73% cells in vehicle treated control (Fig. 1C, upper row). Previous report also shows that EGCG causes G_2/M arrest in HeLa cell cycle [12], so the effect of EGCG on HeLa cell cycle is well reproduced in our experimental conditions. When the cells were treated for 48 h with same dose, 32.55% dead population (sub-G_0) was observed instead of G_2/M arrest (Fig. 1C, bottom row). Thus, the result of cell cycle analysis corroborated well with the result of MTT assay.

Since we found G_2/M arrest of HeLa cell cycle in our experimental set up, we further wanted to observe the expression level of p21 protein in EGCG treated cells, because it is known to have major role in the initiation of G_2/M cell cycle arrest. p21 is an inhibitor of cyclin/cyclin-dependent kinase complexes [32]. It can be induced by both p53-dependent and p53-independent mechanisms and is essential for the onset of both G_0/G_1 and G_2/M cell cycle arrest in response to cell damage [32]. In our study we found that treatment of cells with EGCG for 24 h upregulated Cdk-inhibitor p21 in a dose dependent manner as revealed in western blot analysis (Fig. 1D,E). This upregulation of p21 expression supports G_2/M cell cycle arrest observed in flow cytometric analysis, since overexpression of p21 may be associated with enhanced binding of p21 with G_2 chekpoint proteins Cdk2 and Cdc2 and thus inhibiting them [33,34].

3.2. EGCG depolymerized cellular microtubule and also prevented microtubule formation

Since EGCG caused cell cycle arrest at G_2/M phase, we thought that EGCG might have effects on tubulin-microtubule equilibrium,
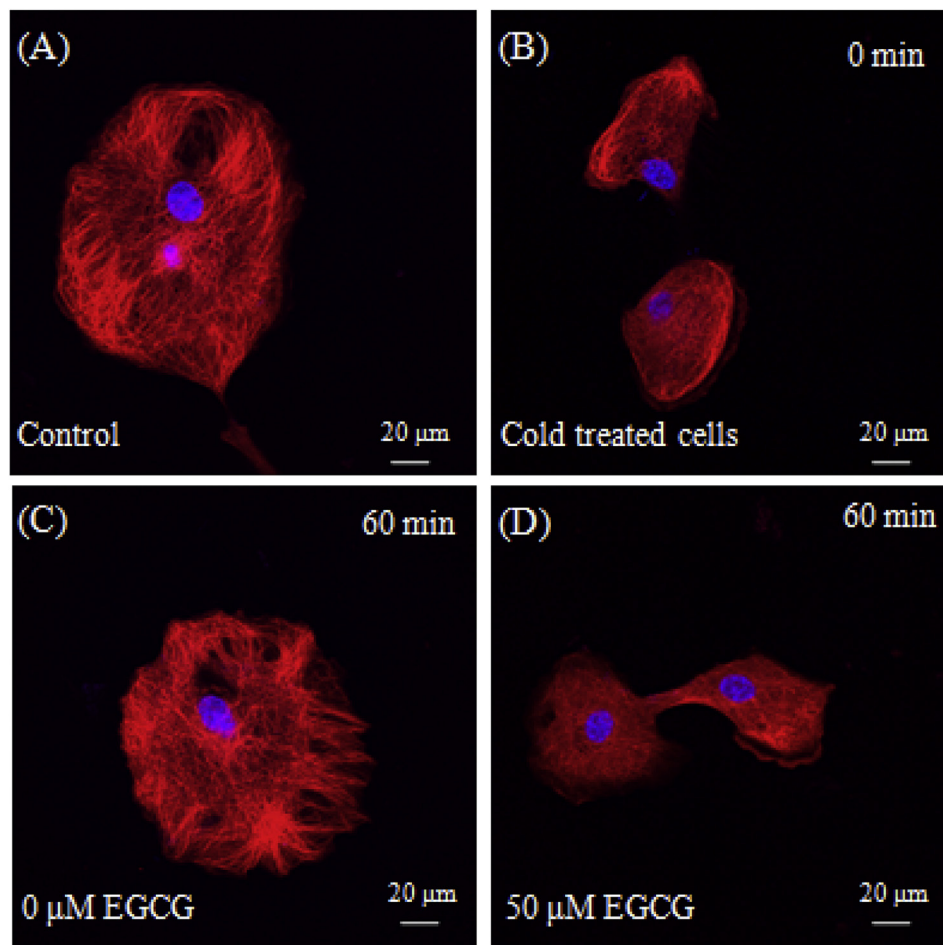
Fig. 3. Immunofluorescence study of reassembly pattern of cold depolymerized interphase microtubule of HeLa cells after replacement with warm media and incubation. (A) and (B) represent cells before and immediate after cold treatment, respectively. (C and D) The reassembly pattern of interphase microtubules of untreated (C) and 50 μM EGCG (D) treated HeLa cells after incubation for 60 min with warm media. Experiment was performed three times with similar result.

because several microtubule targeted ligands are reported to inhibit cell cycle at G_2/M phase. We examined cellular microtubule by confocal microscopic study (Fig. 2) after treating cells with EGCG for 24 h. Control cells (Fig. 2A and B) showed typical interphase microtubule organization. However, 25 μM EGCG (Fig. 2C) started microtubule disruption making the cells contracted. At IC_{50} dose (50 μM) microtubule network was more rapidly disrupted (Fig. 2D) and more higher doses (75 and 100 μM) (Fig. 2E and F) drastically distorted microtubule structure making the cells almost round shaped. These results indicated that EGCG might have depolymerized cellular microtubule. To check the status of other cytoskeleton protein, actin, we treated cells with low doses of EGCG (25 μM) and stained with anti-β-actin antibody. The actin structure of the EGCG treated cells (Fig. 2H) was almost same as that of untreated cells (Fig. 2G). Actin was not that much distorted compared to cellular microtubule at this low dose of EGCG (25 μM). The data of treatment with higher doses of EGCG was not given, because at higher doses actin was also disrupted. It was quite usual since at higher doses of EGCG total cell structure was distorted. Thus we can conclude that at low concentration, EGCG specifically targets microtubule than other cytoskeleton proteins.

To confirm microtubule depolymerization in the presence of EGCG, we performed western blot analysis to measure soluble and polymerized fraction of cellular tubulin of EGCG treated cells (Fig. 2I). We found that 24 h treatment with 50 μM EGCG increased the level of soluble tubulin and decreased the level of assembled tubulin (lane 2) compared to the vehicle treated control cells (Lane 1). The total amount of tubulin was constant. A similar result was observed with colchicine, a known microtubule depolymerizing agent, used as a positive control (Lane 3).

These results confirmed the microtubule depolymerizing effect of EGCG in HeLa cells. More importantly, EGCG started microtubule depolymerization at lower doses and also much before the onset of cell death. For example, 25 μM EGCG (half of the IC_{50} value) was sufficient to disrupt cellular microtubule network within 24 h (Fig. 2C), whereas we found no significant cell death with this dose even after 48 h of treatment (Fig. 1B). Thus the observed G_2/M cell cycle arrest within 24 h might be due to microtubule depolymerization which led to cell death in later hours.

We further tested whether EGCG affected the cellular microtubule formation by observing the reassembly pattern of cold-depolymerized microtubule. At low temperature microtubules (polymers of tubulin dimer) depolymerize into dimeric tubulin and at higher temperature tubulin polymerizes into microtubule. We used this property of tubulin-microtubule system to observe the reassembly pattern of cold-depolymerized cellular microtubule in the presence or absence of EGCG. Cells before cold treatment showed normal interphase microtubule structure (Fig. 3A), and after cold treatment cells became contracted with depolymerized microtubule structure (Fig. 3B). In the absence of EGCG, cold-depolymerized interphase microtubules reassembled to form normal microtubule network within 60 min of incubation at 37 °C
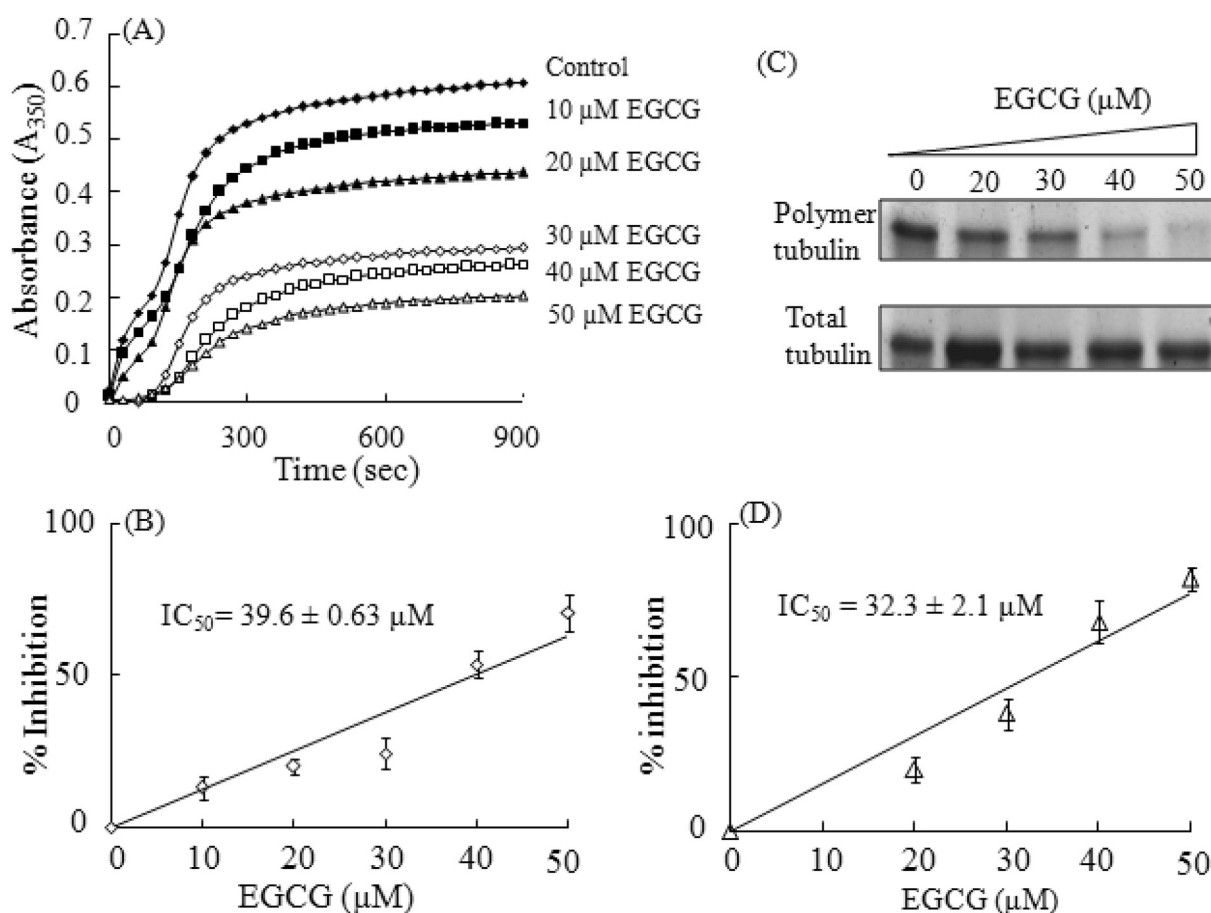
Fig. 4. Inhibition of tubulin assembly by EGCG in vitro. (A) One of the three individual experiments showing the effect of EGCG on microtubule polymerization kinetics, assessed by monitoring the increase in light scattering at 350 nm. (B) Percent of inhibition of polymerization of tubulin with increasing concentration of EGCG with calculated IC_{50} value. Data represents mean ± SD (p < 0.01). (C) SDS-PAGE analysis after in vitro polymerization of tubulin in presence of EGCG (0–50 μM). Polymerized tubulin was pelleted down and stained with coomassie. (D) Percent of decrease in microtubule pellet formation with increasing concentration of EGCG with IC50 value. Data represents mean ± SD (p < 0.01).

with fresh warm media (Fig. 3C). But in presence of EGCG (50 μM) microtubules failed to reassemble at same condition (Fig. 3D). This data suggests that EGCG not only depolymerizes cellular microtubule but also prevents microtubule formation inside cells.

This prevention of microtubule formation was confirmed by study of polymerization of purified tubulin in the presence of EGCG *in cell-free* system and that was monitored by light scattering assay using spectrophotometer. EGCG inhibited both rate and extent of tubulin polymerization in a concentration dependent manner (Fig. 4A) with the IC_{50} value (dose causing 50% inhibition of microtubule polymerization) of 39.6 ± 0.63 μM ($P < 0.01$) (Fig. 4B). This inhibition of tubulin polymerization was also confirmed by analysing microtubule pellets formed in the presence of various concentrations of EGCG. Fig. 4C shows that, with increasing dose of EGCG the amount of microtubule pellet was gradually decreased down. A plot of percent of inhibition of pellet formation against EGCG concentration revealed an IC_{50} value of 32.3 ± 2.1 μM, which was comparable with value found from light scattering assay. These data altogether suggested that EGCG might have interacted with tubulin, altering tubulin-microtubule dynamics, which ultimately resulted in perturbation of cellular microtubule network.

Taken together all the above results we can conclude that, since microtubules are polymers of tubulin heterodimers, there is always equilibrium between tubulin and microtubule in cells and EGCG by binding to tubulin and not to microtubules, shifts the equilibrium towards tubulin dimmers. As a result, microtubules were depolymerized in cells (Fig. 2). Also, the inhibition of polymerization of tubulin into microtubules in cells by EGCG is shown in Fig. 3. Previous reports supports this type of interaction between ligand and tubulin-microtubule equilibrium [18,25,26].

3.3. Binding of EGCG to tubulin

Incubation of tubulin (1 μM) with excess amount of EGCG (20 μM) quenched about 40% tryptophan fluorescence within 30 min at 25 °C (Fig. 5A, B). This decrease of tryptophan fluorescence with time indicated time dependent binding which completed within 30 min at 25 °C. As Fig. 5A shows, EGCG did not alter the λ_{max} of emission wavelength of tubulin, which indicated that the binding did not change the polarity of immediate environment of tryptophan residues. Fig. 5B shows the time dependent quenching of tryptophan fluorescence upon EGCG binding under pseudo-first order condition. The logarithmic plot in Fig. 5C shows fast and slow binding phases when analyzed according to the method of Lambier and Engelborghs [27] and the apparent second order rate constant for the fast phase (k_{on}) was calculated to be 1385 ± 107.65 M^{-1} s^{-1}. Colchicine, a well known tubulin binding drug, shows similar biphasic nature of tubulin binding which arises from its differential binding to β-tubulin isotypes of brain tubulin [35]. Thus EGCG and colchicine may have recognized the same site
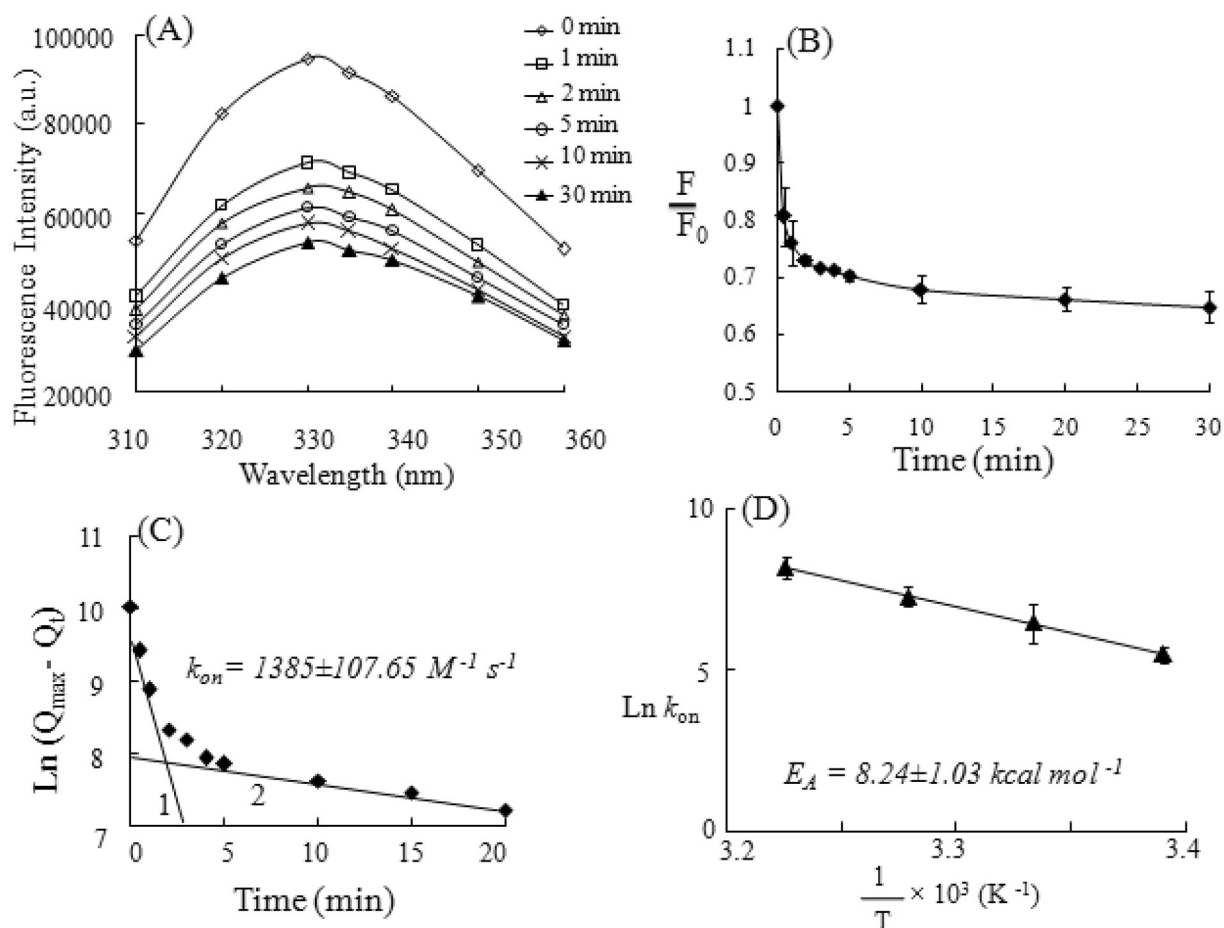
Fig. 5. Kinetics of EGCG binding to tubulin. (A) Fluorescence spectrum of tubulin (1 μM) and EGCG (20 μM) mixture at different time of incubation after exciting at 295 nm. (B) Relative tryptophan fluorescence of tubulin upon binding of EGCG (20 μM) to tubulin (1 μM) with time. (C) The semilogarithmic plot of ln($Q_{max} - Q_t$) versus time. The biphasic plot obtained from one of the three individual experiments was resolved into its component phases. The fast and slow phases are shown as 1 and 2, respectively. The k_{on} value was calculated from three different experiments and represented as mean ± SD ($P < 0.01$). (D) Arrhenius plot with calculated value of activation energy (E_A). Data are represented as mean ± SD ($P < 0.01$) where $n = 3$.

on tubulin and interacted in similar way. We have also calculated the activation energy (E_A) of EGCG-tubulin binding and it was found to be $(+)8.24 \pm 1.03$ kcal mol^{-1} (Fig. 5D).

After determining the kinetic parameters, we were interested to see the affinity of EGCG for tubulin at equilibrium of binding reaction. Fig. 6A shows tryptophan fluorescence quenching pattern with different doses of EGCG. The dissociation constant (K_d) was determined from the double reciprocal plot, taking the binding stoichiometry as 1:1 and the value was found to be 3.5 ± 0.4 μM ($p < 0.01$) (Fig. 6B). Using the observed K_d value we had generated a theoretical curve by GraphPad prism 5 software and the theoretical curve was overlayed with the actual tryptophan fluorescence quenching curve of Fig. 6A. Both the curves are almost overlapping with very little deviation (Fig. 6A inset). We have also performed the scatchard plot analysis to determine the association constant (K_a) (Fig. 6B inset) and it was observed to be 0.25 ± 0.05 μM^{-1} with single binding site per tubulin molecule ($n = 1.03 \pm 0.1$).

The stoichiometry of the ligand–protein interaction was further verified using the Job plot analysis as described in materials and methods section. Here also the binding stoichiometry was found to be 1:1 (molar ratio) (Fig. 6C), keeping good agreement with the result obtained from Scatchard analysis.

We also determined different thermodynamic parameters of EGCG-tubulin binding. Fig. 6D shows the van't Hoff plot of EGCG-tubulin binding. The calculated values of ΔH^0 and ΔS^0 were $(+)$ 3.73 ± 0.45 kcal mol^{-1} and $(+)$ 18.75 ± 1.48 cal K^{-1} mol^{-1} and ΔG^0 at 25 °C was found to be $(-)$ 1.85 ± 0.013 kcal mol^{-1}. Since we found a positive enthalpy change, the binding is mainly entropy driven.

3.4. EGCG binds close to the colchicines binding site on tubulin

Like colchicine, EGCG also inhibited tubulin polymerization and also depolymerized preformed microtubules. So, we examined whether it binds at the colchicine binding site or not. We measured the fluorescence of tubulin-colchicine complex at 430 nm in the presence of different concentrations of EGCG. EGCG inhibited colchicine binding to tubulin in a concentration dependant manner, although the extent of inhibition was not that much found in case of other colchicine site binding drugs. For example, 50 μM EGCG inhibited colchicine binding to tubulin only by 10% (Fig. 7A). In silico study also revealed that in most stable condition EGCG was bound to α-subunit of tubulin near colchicine binding site at the interphase of two subunits (Fig. 7B, C). Further study revealed that the binding of EGCG to tubulin was governed by H1 and H2 helix and its associated loops of N-terminal domain and H7 helix of intermediate domain of α subunit. Furthermore H7, H8, and H10 helix, B8 beta sheet, T7 loops of intermediate domain of β subunit were also found to be involved in binding with EGCG (Fig. 7D). Several non covalent interactions, including H-bonding, were responsible for EGCG binding to those domains of tubulin.
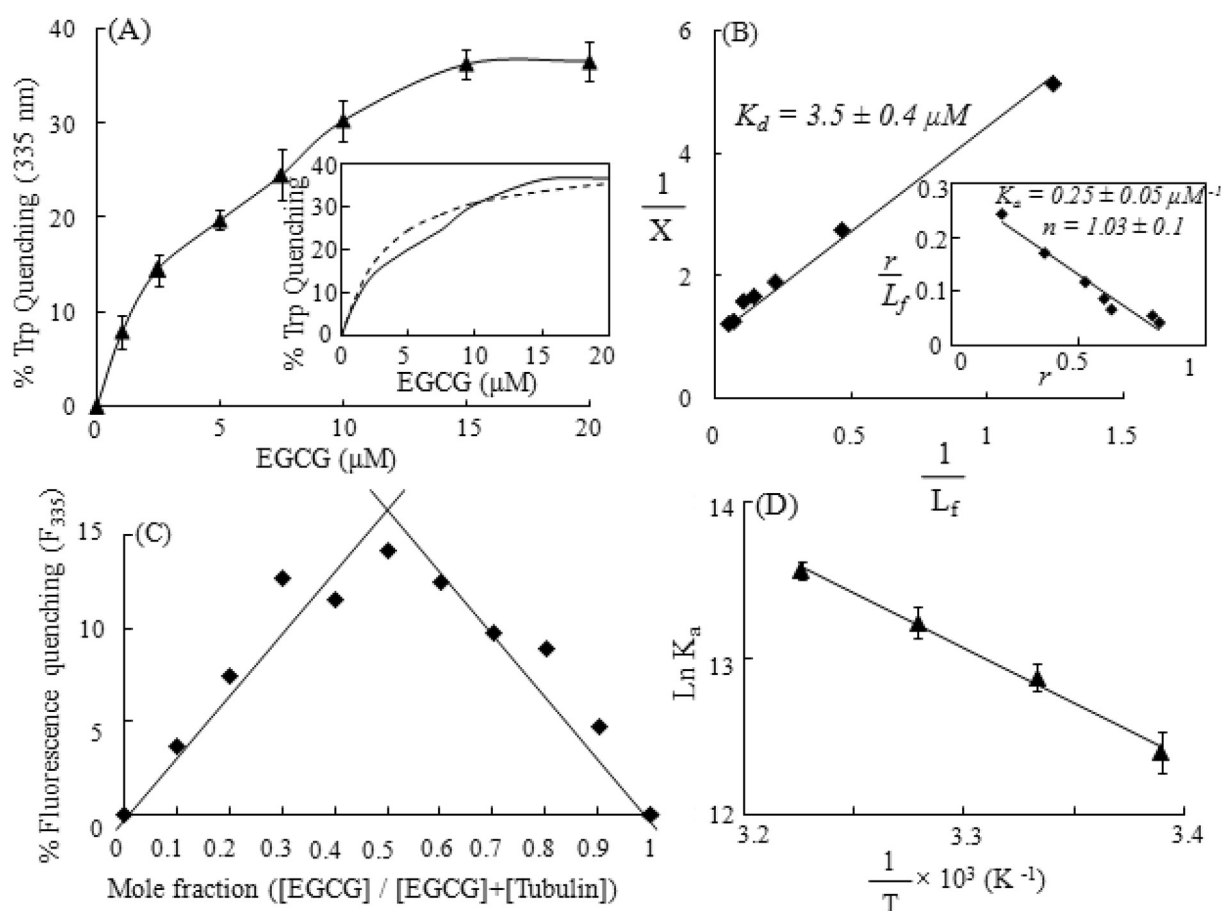
Fig. 6. Binding of EGCG to tubulin was assessed by fluorescence spectroscopy. (A) Percent of tryptophan fluorescence quenching of tubulin (1 μM) in presence of EGCG (0–20 μM). In inset, the theoretical curve of tubulin-EGCG binding of K_d 3.5 μM (dotted line) and the original experimental curve (solid line). (B) Double-reciprocal plot for binding of EGCG to tubulin. Data are representative of three identical experiments. K_d is represented as mean ± SD ($p < 0.01$). In inset, Scachard analysis of EGCG binding to tubulin. K_a and n were determined from three data sets and represented as mean ± SD ($P < 0.01$). (C) Job plot for binding of EGCG to tubulin. Data represents one of three similar experiments. (D) van't Hoff plot of EGCG binding to tubulin. Data are representative of three identical experiments and expressed as mean ± SD.
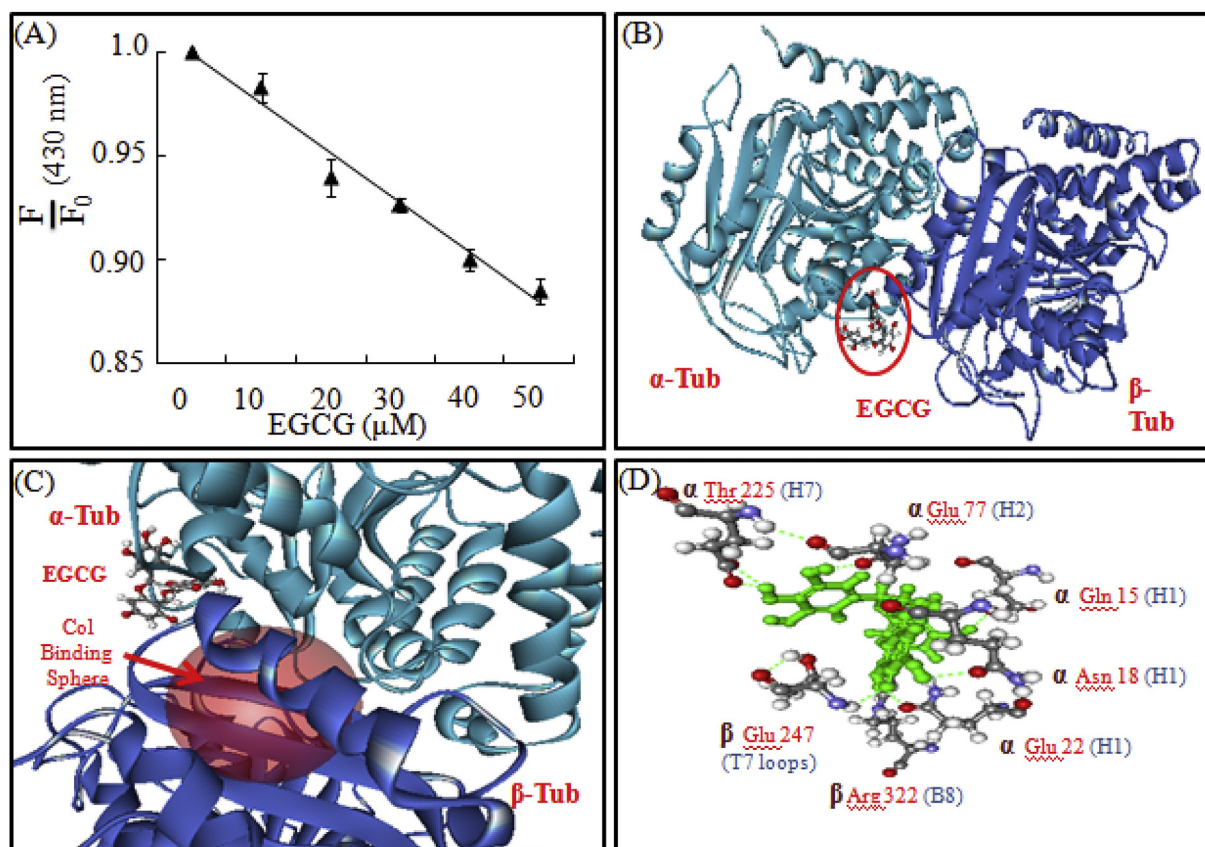
Fig. 7. Determination of binding site of EGCG on tubulin. (A) Change of relative fluorescence of colchicines—tubulin complex at 430 nm with increasing concentration of EGCG. (B—D) *In silico* prediction of binding site of EGCG on tubulin. (B) Binding of EGCG (shown within red circle) on tubulin heterodimer. In the ribbon diagram cyan stands for α-tubulin monomer and blue stands for β-tubulin monomer. (C) Binding of EGCG near the colchicine binding site (red sphere) in tubulin heterodimer. (D) Ball and stick model showing hydrogen bonds between EGCG and different amino acids of surrounding helices and loops at the most stable binding condition. (For interpretation of the references to colour in this figure legend, the reader is referred to the web version of this article.)

Importantly, it was found that these interacting domains of β-subunit (like H7, H8 and T7 loops) were also involved in the colchicine binding [36,37]. So it was possible that binding of EGCG to tubulin may hinder binding of colchicine to tubulin surface, what we found in our biophysical data. Therefore, we concluded that EGCG bound near colchicine binding site which was not completely overlapping with colchicine site on tubulin and that explained small amount of decrease in colchicine-tubulin fluorescence (10%) in the presence of EGCG.

4. Conclusion

In the present study the antiproliferative activity of EGCG has been correlated to its ability to depolymerize microtubule through tubulin binding. Although EGCG binds very close to the colchicine binding site on tubulin, its IC_{50} value for cells under culture condition is 1000 fold higher than colchicine. The reason may be that the local concentration of EGCG inside cells for reaction with tubulin-microtubule is low. This may be due to the fact that EGCG has many other activities in cells [1—6]. For this reason it can be used in combination with other microtubule targeted drugs for better chemotherapy. For example, previous report shows that EGCG sensitized breast cancer cells to paclitaxel in murine model [38]. In addition, further research is necessary regarding its specificity toward particular type of tumor and its persistence at that site under *in vivo* condition, because the serum concentration of EGCG after ingestion of green tea is much lower than its effective dose for

cells at culture condition. Upto this study it can be stated that EGCG can be used as lead compound for developing potential anti-mitotic as well as an anti cancer agent.

Transparency document

Transparency document related to this article can be found at http://dx.doi.org/10.1016/j.cbi.2015.11.004.

Appendix A. Supplementary data

Supplementary data related to this article can be found at http://dx.doi.org/10.1016/j.cbi.2015.11.004.

References

[1] C.S. Yang, J.D. Lambert, J. Ju, G. Lu, S. Sang, Tea and cancer prevention: molecular mechanisms and human relevance, Toxicol. Appl. Pharmacol. 224 (2007) 265—273.
[2] C.S. Yang, J.D. Lambert, Z. Hou, J. Ju, G. Lu, X. Hao, Molecular targets for the cancer preventive activity of tea polyphenols, Mol. Carcinog. 45 (2006)

431—435.

[3] R.L. Thangapazham, A.K. Singh, A. Sharma, J. Warren, J.P. Gaddipati, R.K. Maheshwari, Green tea polyphenols and its constituent epigallocatechin gallate inhibits proliferation of human breast cancer cells in vitro and in vivo, Cancer Lett. 245 (2007) 232—241.

[4] J.H. Lee, Y.J. Jeong, S.W. Lee, D. Kim, S.J. Oh, H.S. Lim, H.K. Oh, S.H. Kim, W.J. Kim, J.Y. Jung, EGCG induces apoptosis in human laryngeal epidermoid carcinoma Hep2 cells via mitochondria with the release of apoptosis-inducing factor and endonuclease G, Cancer Lett. 290 (2010) 68—75.

[5] S. Qanungo, M. Das, S. Haldar, A. Basu, Epigallocatechin-3-gallate induces mitochondrial membrane depolarization and caspase-dependent apoptosis in pancreatic cancer cells, Carcinogenesis 26 (2005) 958—967.

[6] S. Liu, X.J. Wang, Y. Liu, Y.F. Cui, PI3K/AKT/mTOR signaling is involved in (-)-epigallocatechin-3-gallate-induced apoptosis of human pancreatic carcinoma cells, Am. J. Chin. Med. 41 (2013) 629—642.

[7] R. Yamauchi, K. Sasaki, K. Yoshida, Identification of epigallocatechin-3-gallate in green tea polyphenols as a potent inducer of p53-dependent apoptosis in the human lung cancer cell line A549, Toxicol. Vitro 23 (2009) 834—839.

[8] N. Khan, F. Afaq, M. Saleem, N. Ahmed, H. Mukhtar, Targeting multiple signaling pathways by green tea polyphenol (-)-epigallocatechin-3-gallate, Cancer Res. 66 (2006) 2500—2505.

[9] M.E. Cavet, K.L. Harrington, T.R. Vollmer, K.W. Ward, J.Z. Zhang, Anti-inflammatory and anti-oxidative effects of the green tea polyphenol epigallocatechin gallate in human corneal epithelial cells, Mol. Vis. 17 (2011) 533—542.

[10] Y.D. Jung, L.M. Ellis, Inhibition of tumour invasion and angiogenesis by epigallocatechin gallate (EGCG), a major component of green tea, Int. J. Exp. Pathol. 82 (2001) 309—316.

[11] B.J. Monk, T.J. Herzog, The evolution of cost-effective screening and prevention of cervical carcinoma: implications of the 2006 consensus guidelines and human papillomavirus vaccination, Am. J. Obstet. Gynecol. 197 (2007) 337—339.

[12] Y. Qiao, J. Cao, L. Xie, X. Shi, Cell growth inhibition and gene expression regulation by (-)-epigallocatechin-3-gallate in human cervical cancer cells, Arch. Pharm. Res. 32 (2009) 1309—1315.

[13] O. Tudoran, O. Soritau, O. Balacescu, L. Balacescu, C. Braicu, M. Rus, C. Gherman, P. Virag, F. Irimie, I.B. Neagoe, Early transcriptional pattern of angiogenesis induced by EGCG treatment in cervical tumour cells, J. Cell. Mol. Med. 16 (2012) 520—530.

[14] C. Sharma, Q.E.A. Nusri, S. Begum, E. Javed, T.A. Rizvi, A. Hussain, (-)-Epigallocatechin-3-gallate induces apoptosis and inhibits invasion and migration of human cervical cancer cells, Asian Pac. J. Cancer Prev. 13 (9) (2012) 4815—4822.

[15] M.A. Jordan, L. Wilson, Microtubules as a target for anticancer drugs, Nat. Rev. Cancer 4 (2004) 253—265.

[16] B. Bhattacharyya, D. Panda, S. Gupta, M. Banerjee, Anti-mitotic activity of colchicine and the structural basis for its interaction with tubulin, Med. Res. Rev. 28 (2008) 155—183.

[17] K.K. Gupta, S.S. Bharne, K. Rathinasamy, N.R. Naik, D. Panda, Dietary antioxidant curcumin inhibits microtubule assembly through tubulin binding, FEBS J. 273 (2006) 5320—5332.

[18] K. Gupta, D. Panda, Perturbation of microtubule polymerization by quercetin through tubulin binding: a novel mechanism of its antiproliferative activity, Biochemistry 41 (2002) 13029—13038.

[19] T. Mosmann, Rapid colorimetric assay for cellular growth and survival: application to proliferation and cytotoxicity assays, J. Immunol. Methods 65 (1983) 55—63.

[20] S. Chakrabarty, A. Das, A. Bhattacharya, G. Chakrabarti, Theaflavins depolymerize microtubule network through tubulin binding and cause apoptosis of cervical carcinoma HeLa cells, J. Agric. Food Chem. 59 (2011) 2040—2048.

[21] A.M. Minotti, S.B. Barlow, F. Cabral, Resistance to antimitotic drugs in Chinese hamster ovary cells correlates with changes in the level of polymerized tubulin, J. Biol. Chem. 266 (1991) 3987—3994.

[22] M.M. Bradford, A rapid and sensitive method for the quantitation of microgram quantities of protein utilizing the principle of protein-dye binding, Anal. Biochem. 72 (1976) 248—254.

[23] E. Hamel, C.M. Lin, Glutamate-induced polymerization of tubulin: characteristics of the reaction and application to the large-scale purification of tubulin, Arch. Biochem. Biophys. 209 (1981) 29—40.

[24] F. Gaskin, C.R. Cantor, M.L. Shelanski, Turbidimetric studies of the in vitro assembly and disassembly of porcine neurotubules, J. Mol. Biol. 89 (1974) 737—755.

[25] B.R. Acharya, D. Chaudhury, A. Das, G. Chakrabarti, Vitamin K3 disrupts the microtubule networks by binding to tubulin: a novel mechanism of its antiproliferative activity, Biochemistry 48 (2009) 6963—6974.

[26] B.R. Acharya, B. Bhattacharyya, G. Chakrabarti, The natural naphthoquinone plumbagin exhibits antiproliferative activity and disrupts the microtubule network through tubulin binding, Biochemistry 47 (2008) 7838—7845.

[27] A. Lambeir, Y. Engelborghs, A fluorescence stopped flow study of colchicine binding to tubulin, J. Biol. Chem. 256 (1981) 3279—3282.

[28] B. Bhattacharyya, S. Kapoor, D. Panda, Fluoresecence spectroscopic methods to analyze drug-tubulin interactions, in: L. Wilson, J.J. Correia (Eds.), Microtubules : In Vitro, Chapter 17, Methods in Cell Biology 95, 2010, pp. 301—329.

[29] C.Y. Huang, Determination of binding stoichiometry by the continuous variation method: the Job plot, Methods Enzymol. 87 (1982) 509—525.

[30] J.S. Yang, M.J. Hour, W.W. Huang, K.L. Lin, S.C. Kuo, J.G. Chung, MJ-29 inhibits tubulin polymerization, induces mitotic arrest, and triggers apoptosis via cyclin-dependent kinase 1-mediated Bcl-2 phosphorylation in human leukemia U937 cells, J. Pharmacol. Exp. Ther. 334 (2010) 477—488.

[31] D. Chaudhury, A. Ganguli, D.G. Dastidar, B.R. Acharya, A. Das, G. Chakrabarti, Apigenin shows synergistic anticancer activity with curcumin by binding at different sites of tubulin, Biochimie 95 (2013) 1297—1309.

[32] I. Roninson, Oncogenic functions of tumour suppressor p21Waf1/Cip1/Sdi1: association with cell senescence and tumour-promoting activities of stromal fibroblasts, Cancer Lett. 179 (2002) 1—14.

[33] Y. Gu, C.W. Truck, Inhibition of Cdk2 activity in vivo by an associated 20 K regulatory subunit, Nature 366 (1993) 707—710.

[34] Y.H. Choi, W.H. Lee, K.Y. Park, L. Zhang, p53 independent induction of p21 (WAF1/CIP1), reduction of cyclin B1 and G2/M arrest by the isoflavone genistein in human prostate carcinoma cells, Jpn. J. Cancer Res. 91 (2000) 164—173.

[35] A. Banerjee, R.F. Luduena, Kinetics of association and dissociation of colchicine-tubulin complex from brain and renal tubulin. Evidence for the existence of multiple isotypes of tubulin in brain with differential affinity to colchicine, FEBS Lett. 219 (1987) 103—107.

[36] R.B. Ravelli, B. Gigant, P.A. Curmi, I. Jourdian, S. Lachkar, A. Sobel, M. Knossow, Insight into tubulin regulation from a complex with colchicine and a stathmin-like domain, Nature 428 (2004) 198—202.

[37] A. Dorleans, B. Gigant, R.B. Ravelli, P. Mailliet, V. Mikol, M. Knossow, Variations in the colchicine-binding domain provide insight into the structural switch of tubulin, Proc. Natl. Acad. Sci. U. S. A. 106 (2009) 13775—13779.

[38] T. Luo, J. Wang, Y. Yin, H. Hua, J. Jing, X. Sun, M. Li, Y. Zang, Y. Jiang, (-)-Epigallocatechin gallate sensitizes breast cancer cells to paclitaxel in a murine model of breast carcinoma, Breast Cancer Res. 12 (1) (2010) R8.